J Appl Electrochem (2009) 39:1393–1397
DOI 10.1007/s10800-009-9816-3

ORIGINAL PAPER

Pulsed electrodeposition of microcrystalline chromium from trivalent Cr-DMF bath

G. Saravanan · S. Mohan

Received: 5 November 2008 / Accepted: 26 January 2009 / Published online: 17 February 2009

Abstract Pulsed electrodeposition (PED) with square wave has successfully been applied to deposit microcrystalline chromium from Cr-dimethylformamide (DMF) bath. The influence of the duty cycle, on-time, off-time, frequency, and pulse peak current on thickness, current efficiency, and hardness were investigated. Based on the analysis of the microstructure, the corrosion behavior of both direct-current deposited (DCD) and pulse-current deposited (PED) chromium in 3.5% NaCl solution was studied using potentiodynamic polarization and electrochemical impedance spectroscopy (EIS). The results indicated that both pulsed electrodeposits and direct-current deposits have high charge transfer resistance R_{ct} and very low I_{corr} compared with mild-steel substrate.

Keywords Trivalent chromium · Chromium electrodeposition · Duty cycle · Coatings · Electrochemical impedance spectroscopy (EIS) · Porosity

1 Introduction

Electrodeposition of chromium is carried out in aqueous solution containing Cr(III) ions as a metal component for anticorrosion surface modification of suitable substrate using square-wave pulsed electrolysis. Shunsuke Yagi et al. [1] recently reported formation of Fe–Cr alloy through pulsed electrodeposition. Pulse plating can be defined as current-interrupted electroplating. Figure 1 shows a typical oscilloscope trace of a square-wave attainable with existing pulse equipment. However, the figure does not show a pure square-wave because there is a gradual curvature to both the ascending and descending current flows. The curvature on the rising flow is intentionally induced electronically to avoid an instantaneous rise and current overshoot. This type of pulse process is suggested as a means of obtaining smooth and bright deposits. If, for example, the duty cycle flows for 40 ms and is interrupted for 60 ms between periods of flow, there is greater opportunity for replenishment of the cathode film through diffusion and convection. Cathode polarization is increased, and cathode efficiency may be increased. Consequently, a high current density can be used and a desired thickness can be deposited in shorter time, even though the current is not flowing continuously. In pulse electrolysis, selection of the electrolyte, peak current density, on-time, and off-time determines the physical characteristics of the deposits [2]. Chromium plating is widely applied in various fields such as aerospace, automotive, and general engineering industries, since chromium plating has excellent abrasion resistance, corrosion resistance [3], and hardness. Chromium was first deposited from hexavalent chromic acid solution by Geuther 150 years ago [4]. Later, plating solutions based on chromic acid were investigated and produced on a commercial basis [5, 6]. Improvement in surface appearance and mechanical properties has also been reported using normal pulsed electrolysis with regard to Cr [7] and Cr alloy plating [8, 9]. However, chromium plating from Cr(VI) solution is now under pressure due to its toxicity and carcinogenicity; therefore, significant efforts have been applied to the development of alternative process for chromium plating from Cr(VI) solution [10, 11]. The present work was also important in terms of a Cr(VI)-free process, using Cr(III) solution as an alternate bath.

G. Saravanan · S. Mohan (✉)
Central Electrochemical Research Institute,
Karaikudi 630006, India
e-mail: sanjnamohan@yahoo.com

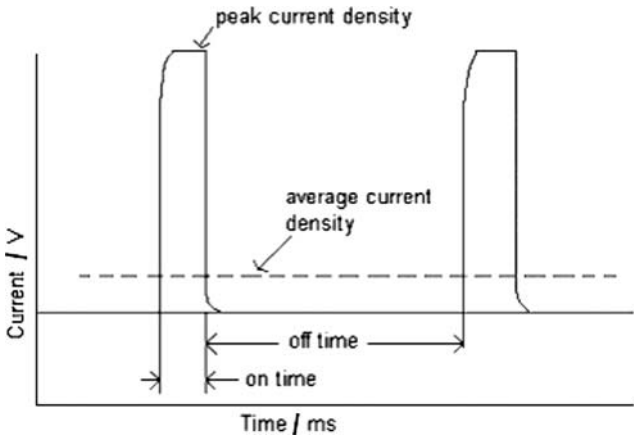

Fig. 1 Square-wave pulsed current with curved flow

2 Experimental

2.1 Materials preparation

Electrodeposited chromium was prepared from a dimethylformamide bath consisting of 212 g L^{-1} $CrCl_3 6H_2O$, 26 g L^{-1} NH_4Cl, 36 g L^{-1} NaCl, 20 g L^{-1} $B(OH)_3$, and 189.4 g L^{-1} (200 mL L^{-1}) dimethylformamide. AR-grade chemicals and distilled water were used to prepare the solution. Electrodeposits with thickness of about 7 μm were obtained at average current density of 15 A dm^{-2} in 10 min. The solution was maintained at pH 2 ± 0.2 and temperature 30 ± 1 °C, and stirred by mechanical stirrer. Graphite and brass plates were used as the anode and cathode, respectively. The samples obtained for mild steel, DC-deposited chromium, and PE-deposited chromium are represented by (MS), Cr-(DCD)/MS, and Cr-(PED)/MS respectively. Pulse plating was done using Dynatronix (USA) model DPR 20-5-10. Surface morphologies of electrodeposits were characterized by scanning electron microscopy (SEM) employing a Hitachi 3000H. Crystallite size was assessed by X-ray diffraction (XRD) technique using a Phillips diffractometer with Cu*K* (2.2 kW maximum) as source. Crystallite size was calculated using Debye-Sherrer formula.

2.2 Corrosion measurements

2.2.1 Cell apparatus

Corrosion measurements were performed in a three-electrode cell with volume of 150 mL. (MS), Cr-(DCD)/MS, and Cr-(PED)/MS samples were used as the working electrode (WE). Platinum foil and saturated calomel electrode (SCE) were used as the auxiliary and reference electrode, respectively. The electrodes were connected to a potentiostat (PARSTAT 2273). Corrosion parameters were obtained with built-in software package (powerCORR). All potentials in this work are referred to SCE.

2.2.2 Electrochemical procedures

Corrosion behavior was examined in neutral 3.5% NaCl solution at 30 ± 1 °C. Potentiodynamic polarization curves were measured for all the samples between −0.8 and −0.2 V at scan rate of 5 mV s^{-1}. Impedance spectra were conducted at open-circuit potential over a frequency range from 10^5 to 10^{-2} Hz. The amplitude of potential modulation was 5 mV. All the recorded impedance spectra were shown as Bode diagram.

3 Results and discussion

3.1 Effect of duty cycle on thickness, current efficiency, and hardness of Cr deposits

Figure 2a shows the effect of pulse duty cycle on the thickness of Cr deposits obtained for various frequencies at average current density of 15 A dm^{-2}. From this figure, it is observed that the thickness of the chromium deposit increases with increasing pulse duty cycle. As the duty cycle increases, current on-time increases and off-time decreases. At lower duty cycle, the peak current is flowing for less time and so the overall amount of deposition is less than for higher duty cycle. Also at very high duty cycle and high frequencies the pulse current is very low, and so correspondingly reduced thickness is obtained. The maximum thickness of 7.3 μm was obtained at 40% duty cycle for lower pulse frequencies (10 and 25 Hz) at current density of 15 A dm^{-2} [12].

Figure 2b shows the effect of pulse duty cycle on current efficiency of Cr deposits obtained for various frequencies at its average current density of 15 A dm^{-2}. The maximum current efficiency is obtained at 40% duty cycle at lower pulse frequencies (25 and 50 Hz). As pulse frequency increases, the pulses are very short and they produce very thin pulse diffusion layers. Diffusion of metal ions from the bulk of electrolyte to the electrode surface depends on gradient of metal ions concentration. So at 40% duty cycle at lower pulse frequencies enhancement of migration of ions increases the nucleation rate, uniformity of deposit [13], and deposition rate, and hence current efficiency is increased.

Figure 2c shows the effect of pulse duty cycle on the hardness of Cr deposits obtained for various frequencies at average current density of 15 A dm^{-2}. The hardness of the Cr deposit was found to increase with increase of duty cycle [14]. A maximum hardness value was obtained at 40% duty cycle at low frequencies (10 and 25 Hz) when

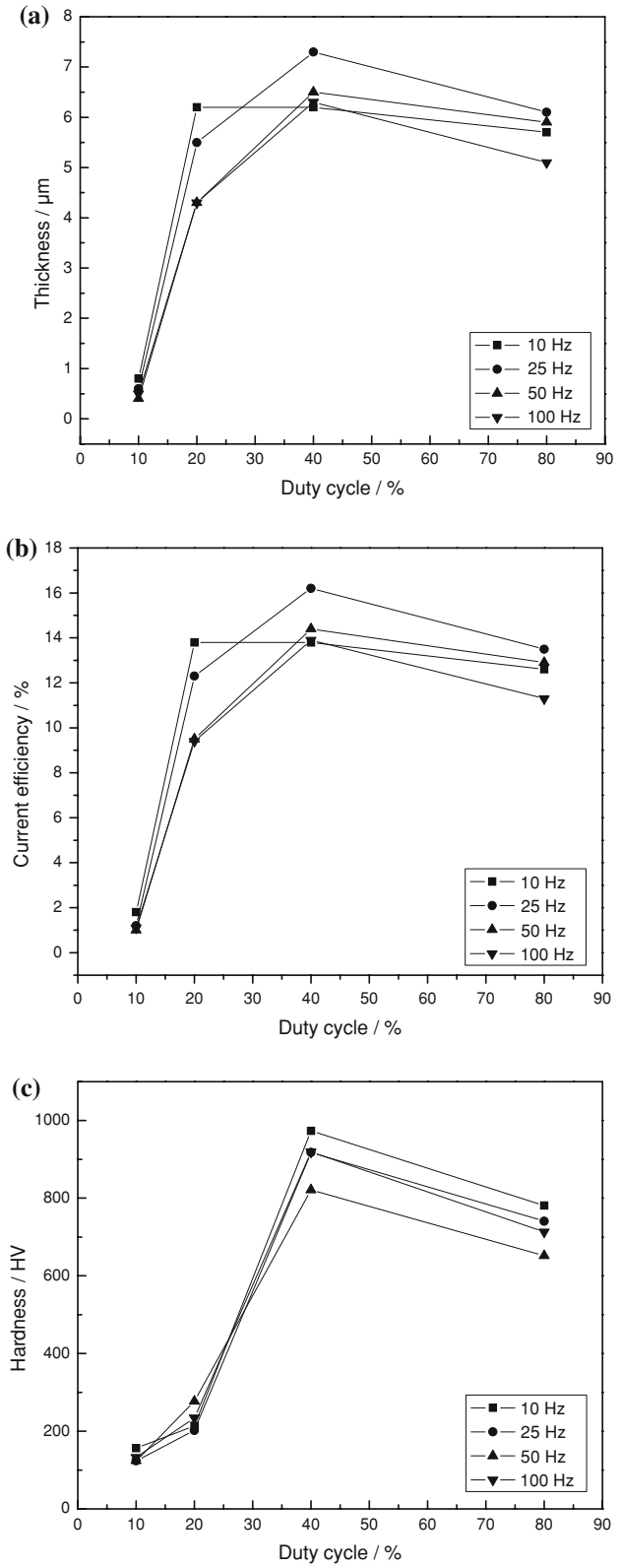

Fig. 2 Effect of duty cycle on: **a** thickness, **b** current efficiency, and **c** hardness of deposit

the average current density was 15 A dm^{-2}. Because at low pulse duty cycle a high peak current is passed, this produces powdery or burnt deposits with poor adhesion and considerable porosity. This porosity leads to a decrease in hardness of the deposit. However, at 40% duty cycle, the peak current is lower due to the formation of a smooth fine-grained deposit. Improved surface coverage with denser built-up of grains is to be expected [2]. At higher frequencies (100 Hz) the pulse current appears to be almost equal to that of DC deposition because there is no sufficient relaxation time for re-establishment of equilibrium between the ions in the bulk solution and the electrode surface, which leads to the formation of porous deposit. So hardness of the deposit decreases beyond 40% duty cycle.

3.2 Microstructural characteristics

Morphology of chromium deposits on brass substrate was examined under scanning electron microscopy (SEM). Figure 3a shows a SEM photograph of the chromium deposit obtained after 10 min with 40% duty cycle at average current density of 15 A dm^{-2}. The deposits exhibited columnar [15] nodular structures with nodular size ranging from 3 to 8 µm. Deposits were brighter and smoother with microcracks. The decreased porosity and denser packed surface are due to the desorption of hydrogen during the off-time of the pulse cycle.

The XRD patterns of electrodeposited chromium are shown in Fig. 3b. All the electrodeposits consist of grains with weak Cr(110) plane and strong Cu(200), Cu(220) plane due to lower thickness (less than 16 µm) of chromium coatings. Crystallite size of Cr(110) at 10%, 20%, and 40% duty cycle are 31.9, 51.1, and 63.9 nm, respectively. When duty cycle increases, on-time increases and off-time decreases and this leads to insufficient supply of reacting species and hence reduced nucleation rate and increased grain size during electrodeposition. It has been reported [16] that coarse-grained electrodeposition due to concentration depletion occurred as on-time increased. A large grain size therefore results from the evolution of more hydrogen at the cathode interface [17].

3.3 Corrosion examinations

3.3.1 Potentiodynamic polarization tests

Figure 4a shows potentiodynamic polarization curves for electrodeposited chromium in 3.5% NaCl solution. All the curves display active-passive behavior between −0.8 and −0.2 V. This indicates that the mechanism of activity and

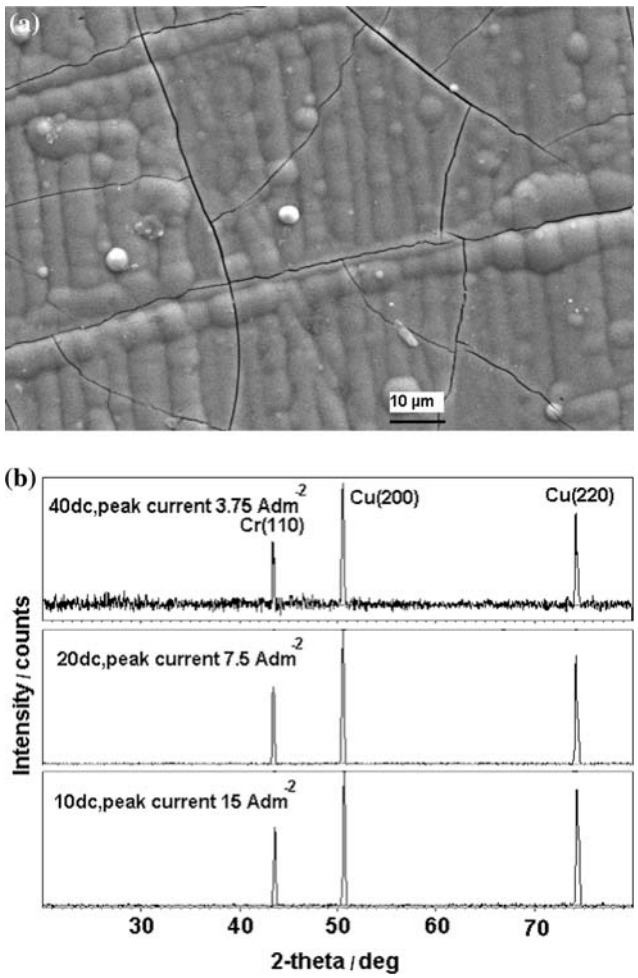

Fig. 3 **a** Scanning electron microscopy (SEM) of chromium deposits at 40% duty cycle at peak current density of 3.7 A dm^{-2}. **b** XRD patterns of chromium deposited chromium prepared at different duty cycles

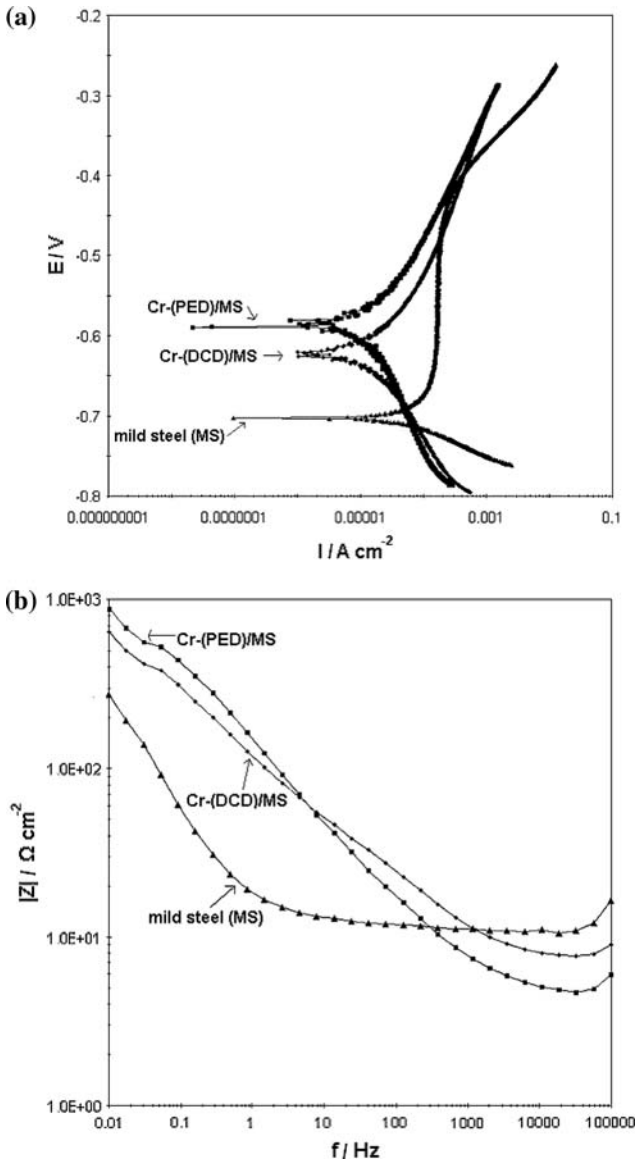

Fig. 4 **a** Polarization curve of electrodeposited chromium in 3.5% NaCl solution. Impedance spectra for electrodeposited chromium in 3.5% NaCl solution. **b** Bode diagram

passivation is similar in essence for all electrodeposits. The current density increases with increasing potential at the activation region, then the electrode passivates and displays high stability, as characterized by a low and steady value of passive current density. The corrosion current density (I_{corr}) and corrosion potential (E_{corr}) are calculated from the intercept of the Tafel slops. The corrosion rate (CR) in mills per year was estimated from the polarization curves, and is tabulated in Table 1. Among all the samples Cr-(PED)/MS exhibits the lowest values of I_{corr} and CR than that of samples Cr-(DCD)/MS and mild steel (MS). Therefore, sample Cr-(PED)/MS exhibits the best corrosion resistance [3], which is attributed to the compact microstructure.

3.3.2 Electrochemical impedance spectra tests

The measured impedance spectra for the electrodeposits in 3.5% NaCl solution are shown as Bode diagrams in Fig. 4b. The equivalent circuit (Fig. 5) is used to fit the corrosion resistance parameters. R_{ct} and C_{dl} represent the charge-transfer resistance and double-layer capacitance, respectively. The fitted impedance spectra are in good agreement with the impedance spectra recorded during the measurements, as shown in Fig. 4. The calculated values of circuit elements are listed in Table 1. It can be found that all fitted corrosion parameters of the electrodeposits vary with the changes of the microstructure. The corrosion resistance (R_{ct}) of PED chromium (C) is greater than that of other samples. The increased R_{ct} values and decreased C_{dl} values for Cr deposits clearly confirm the better corrosion resistance of these PED and DC deposit compared with bare mild-steel substrates.

Table 1 Corrosion parameters obtained from polarization studies and impedance measurements by Bode and Nyquist plots in 3.5% w/v NaCl solution

Sample	E_{corr} vs. SCE (V)	b_a (V dec^{-1})	b_c (V dec^{-1})	I_{corr} (A cm^{-2})	Corrosion rate (mpy)	OCP (V)	R_{ct} (Ω cm^{-2})	C_{dl} (F cm^{-2})
MS panel	−0.702	0.483	−0.043	8.5×10^{-5}	3.9×10^{1}	−0.511	263	0.060
Cr on MS (DC)	−0.620	0.279	−0.157	8.3×10^{-5}	2.6×10^{1}	−0.545	654	0.049
Cr on MS (PC)	−0.589	0.145	−0.181	1.4×10^{-5}	4.6	−0.537	1006	0.014

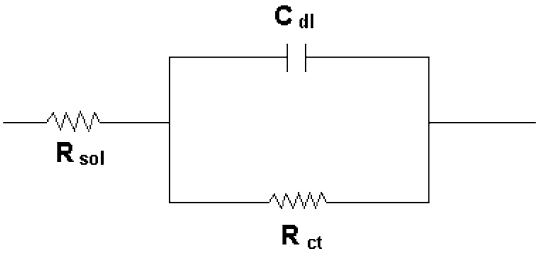

Fig. 5 Equivalent circuit diagram of impedance spectra for electrodeposited chromium in 3.5% NaCl solution

3.3.3 Porosity of Cr-(DCD) and Cr-(PED) systems

It is possible to determine the porosity of a coating using an electrochemical measurement technique that determines the ratio of the current density through the pores and the coating [18]. Elsener et al. [19] estimated the porosity of TiN coated mild steel from the shift of the corrosion potential caused by the presence of the coating (ΔE_{corr}) and from the individual polarization resistance of the coatings (R_p) and the substrate materials ($R_{p,s}$) as given below [6].

$$P = \left(\frac{R_{p,s}}{R_p}\right) \times 10^{-|\Delta E_{CORR}|/b_a}$$

where b_a is the Tafel slope of the active dissolution of mild steel.

Using this equation, and the values of $R_{p,s} = 263\ \Omega\ cm^2$ and $b_a = 0.483$ V decade^{-1}) determined from separate measurement on an uncoated mild steel (MS) substrate in 3.5% NaCl solution, we estimated the porosity of the Cr-(DCD) and Cr-(PED) systems. For this purpose E_{corr} of the mild steel was determined to be −702 mV versus SCE. The coating porosity determined in this way was approximately 0.2724% for the Cr(DCD) system and 0.0256% for the Cr (PED) system in 3.5% NaCl solution. From this value the PED Cr coating system had ten times lower porosity than the DCD Cr system. Therefore PED Cr has better corrosion resistance than the DCD Cr coating system.

4 Conclusions

The microstructure and corrosion behavior of electrodeposited chromium prepared at different peak current densities, duty cycles, and frequency were studied. The following conclusion can be drawn: Grain size increases with decreasing peak current density during electrodeposition. The maximum thickness, current efficiency, and hardness of electrodeposited chromium are obtained at 40% duty cycle. All the chromium samples exhibit active-passive polarization characteristics. Electrodeposited chromium prepared at 40% duty cycle exhibited the best corrosion resistance. The corrosion behavior of electrodeposited chromium in 3.5% NaCl solution is well described by the equivalent system of charge-transfer resistance (R_{ct}) and double-layer capacitance (C_{dl}).

Acknowledgements One of the authors (Dr S. Mohan) thanks the Department of Science and Technology New Delhi for a research grant under SERC (Engineering Sciences) scheme no. SR/S3/ME/047/2005.

References

1. Yagi S, Murase K, Hirato T, Awakura Y (2007) J Electrochem Soc 154:D304
2. Puippe JC, Leaman F (1986) Theory and practice of pulse plating, 1st edn. American Electroplaters and Surface Finishers Society, Orland, FL, 247 pp
3. Qui JH (2003) Mater Sci Forum 211:437
4. Kishi M (1986) Hyomen Gijutsu 37:159
5. Selvam M (1983) Met Finish 81:7
6. Morikawa T, Eguchi S (1986) Hyomen Gijutsu 37:341
7. Saiddington JC (1978) Plat Surf Finish 65:45
8. Eckler TA, Manty BA, McDaniel PL (1980) Plat Surf Finish 67:60
9. Gelchinski MH, Gal-Or L, Yahalom J (1982) J Electrochem Soc 129:2433
10. Hirato T, Terabataka T, Watanabe E, Awakura Y (1996) Hyomen Gijutsu 47:245
11. El-Sharif M (1997) Trans Inst Met Finish 75:143
12. Devaraj G, Seshadri SK (1996) Plat Surf Finish 83(6):62
13. Pearson T, Dennis JK (1990) J Appl Electrochem 20:196–208
14. Pearson T, Dennis JK (1990) Surf Coat Technol 42:69
15. Song YB, Chin D-T (2002) Electrochim Acta 48(4):349
16. Toth-Kadar E, Bakonyi I, Pogany L, Cziraki A (1996) Surf Coat Technol 88:57
17. Ebrahimi F, Ahmed Z (2003) J Appl Electrochem 33:733
18. Tato W, Landolt D (1998) J. Electrochem Soc 145:4173
19. Elsener B, Rota A, Bohni H (1989) Mater Sci Forum 29:44